THE ASTROPHYSICAL JOURNAL, 527:600–608, 1999 December 20

TIDALLY COMPRESSED GAS IN CENTERS OF EARLY-TYPE AND ULTRALUMINOUS GALAXIES

MOUSUMI DAS
Raman Research Institute, C. V. Raman Avenue, Bangalore 560 080, India; mousumi@rri.ernet.in
AND
CHANDA J. JOG
Department of Physics, Indian Institute of Science, Bangalore 560012, India; cjjog@physics.iisc.ernet.in
Received 1999 April 16; accepted 1999 July 22

ABSTRACT

In this paper we propose that the compressive tidal field in the centers of flat-core early-type galaxies and ultraluminous galaxies compresses molecular clouds producing dense gas observed in the centers of these galaxies. The effect of galactic tidal fields is usually considered disruptive in the literature. However, for some galaxies, the mass profile flattens toward the center and the resulting galactic tidal field is not disruptive, but instead it is compressive within the flat-core region. We have used the virial theorem to determine the minimum density of a molecular cloud to be stable and gravitationally bound within the tidally compressive region of a galaxy. We have applied the mechanism to determine the mean molecular cloud densities in the centers of a sample of flat-core, early-type galaxies and ultraluminous galaxies. For early-type galaxies with a core-type luminosity profile, the tidal field of the galaxy is compressive within half the core radius. We have calculated the mean gas densities for molecular gas in a sample of early-type galaxies which have already been detected in CO emission, and we obtain mean densities of $\langle n \rangle \sim 10^3$–$10^6$ cm^{-3} within the central 100 pc radius. We also use our model to calculate the molecular cloud densities in the inner few hundred parsecs of a sample of ultraluminous galaxies. From the observed rotation curves of these galaxies we show that they have a compressive core within their nuclear region. Our model predicts minimum molecular gas densities in the range 10^2–10^4 cm^{-3} in the nuclear gas disks; the smaller values are applicable typically for galaxies with larger core radii. The resulting density values agree well with the observed range. Also, for large core radii, even fairly low-density gas ($\sim 10^2$ cm^{-3}) can remain bound and stable close to the galactic center.

Subject headings: galaxies: elliptical and lenticular, cD — galaxies: ISM — galaxies: nuclei

1. INTRODUCTION

Over the last two decades observations have revealed the presence of significant amounts of cold, neutral gas in early-type galaxies (Henkel & Wiklind 1997; Knapp 1998). The term "early-type galaxies" includes lenticular or S0 galaxies, dwarf elliptical (dE), and elliptical (E) galaxies. Many of these galaxies have prominent dust lanes and extended distributions of neutral hydrogen gas (H I). A significant fraction of these galaxies also contains molecular hydrogen gas (H_2). Unlike the H I gas, which is usually distributed in the outer parts of the galaxy, the molecular gas is nearly always centrally concentrated. The H_2 gas in these galaxies has been detected and traced using the CO (1–0) and CO (2–1) lines, indicating that the gas may be fairly dense ($\sim 10^3$ cm^{-3}). In a few cases high-density molecular gas $n(H_2) > 10^4$ cm^{-3} has been observed using the high-density tracers HCN and HCO$^+$. The amount of molecular gas observed in early-type galaxies varies between 10^5 and 10^9 $M_\odot$ and is less than in spirals of the same blue luminosity (Knapp 1998). While the amount of cold gas is small compared to that in spiral galaxies, it is still not insignificant and in some cases also forms the site of ongoing star formation. The origin and spatial distribution of this dense gas has not been explained so far.

Ultraluminous galaxies are very bright starburst galaxies having far-IR luminosities of the order $L > 10^{12}$ $L_\odot$ (Sanders et al. 1988). They are formed from the merger of two gas-rich spiral galaxies. The merger is expected to result in large amounts of disk molecular gas falling into the center of the newly formed merger remnant, which subsequently results in enhanced star formation or superstarburst at the center. The total central gas mass is $\sim 10^9$–10^{10} $M_\odot$ and is distributed over the central few hundred parsecs.

It may seem strange at first that we are studying seemingly different kinds of galaxies (early-type galaxies and ultraluminous galaxies) together in this paper. However, as we argue next, these are close in terms of their dynamics. Mergers of two spirals are known to result in an ultraluminous galaxy, as seen from observations (Sanders et al. 1988), and as explained theoretically (e.g., Jog & Das 1992). A merging pair is believed to be a precursor of an elliptical galaxy, as shown observationally (e.g., Schweizer 1999), and in fact the K-band brightness profiles of about 50% of the ultraluminous galaxies display a $r^{1/4}$ distribution typical of an elliptical galaxy (Sanders & Mirabel 1996). Numerical simulations have shown that a merger of two spirals can result in an elliptical galaxy (e.g., Barnes & Hernquist 1992). This scenario is supported by the fact that the observed gas surface density in the centers of ultraluminous galaxies is 500 $M_\odot$ pc^{-3} and is comparable with the central stellar density in ellipticals (Kormendy & Sanders 1992; Solomon 1997). Therefore, we expect that the mass distribution and, hence, the dynamics of the centers of these galaxies would be similar. Also, the gas number densities would be affected in a similar way by the galactic tidal field. Hence, we study the origin of the dense gas in the centers of early-type and ultraluminous galaxies together in this paper. We do not, however, study the relevance of the compressive tidal field, which we discuss next, for the evolution from a merging pair of spirals into an elliptical galaxy.

The galactic tidal field is usually thought to be disruptive in the centers of galaxies so that only dense gas would survive the strong shearing due to a central tidal field. However, if the potential flattens instead of peaking toward the center of the galaxy, the tidal field can reverse sign and become compressive. The tidal field is compressive when the background gravitational field of the galactic disk enhances the self-gravitational field of the cloud (Binney & Tremaine 1987, chap. 7). We show this situation is physically possible in core regions of some galaxies—such as the flat-core early-type and ultraluminous galaxies. This is a new application of the idea of compressive tidal fields, namely, in the astrophysical context of galaxy centers. In the past, the effect of the compressive nature of tidal fields has been studied in the context of disk shocking of globular clusters (Ostriker, Spitzer, & Chevalier 1972), and the tidal effect on a galaxy in the core of a cluster of galaxies (Valluri 1993). The other new feature of our study is the application of compressive fields to a compressible fluid, namely gas, and our calculation of the steady state density of a bound, virialized cloud in the presence of this field.

In §§ 2 and 3, we determine the minimum density of a stable cloud in a compressive tidal field. We have applied these results (§ 4) to the centers of a few flat-core, early-type galaxies in which molecular gas has been detected and also to a sample of ultraluminous galaxies. We have compared our results with the observed gas densities. We thus show that it is the compressive nature of the galactic tidal fields in the centers of these galaxies that naturally leads to the origin of the dense molecular gas observed in these galaxies.

2. EQUILIBRIUM OF A CLOUD IN THE TIDAL FIELD OF A GALAXY

Molecular clouds are generally bound by self-gravity, hence the compressive galactic tidal field plays an important role in the stability of a cloud. In this section we use the galactic tidal field in a spherical potential to derive the net stability criterion for a cloud.

2.1. *Tidal Field*

The components of the tidal field in a spherical potential has been derived in some detail by Cowsik & Ghosh (1987), and Valluri (1993), who studied the effect of the compressive tidal field of a cluster potential on a galaxy. We summarize their results briefly here before applying them to a molecular cloud. For a potential $\Phi(X_i)$ the tidal field components at x_i, where $x_i = X_i - X_{i0}$, are given by

$$\boldsymbol{T}_{\boldsymbol{x}_j} = -\left(\Sigma_i \left.\frac{\partial^2 \Phi}{\partial X_i \partial X_j}\right|_0 x_i\right)\hat{\boldsymbol{x}}_j \,. \tag{1}$$

For a spherical potential $\Phi(R)$ for which the cloud lies along the X-axis so that $X = R$, $Y = Z = 0$, the components of the tidal field at a position (x, y, z) in the coordinate system centered on the cloud are given by

$$T_x = -\left(\frac{\partial^2 \Phi}{\partial R^2}\right)_0 \boldsymbol{x} \,, \tag{2}$$

$$T_y = -\frac{1}{R}\left(\frac{\partial \Phi}{\partial R}\right)_0 \boldsymbol{y} \,, \tag{3}$$

$$T_z = -\frac{1}{R}\left(\frac{\partial \Phi}{\partial R}\right)_0 \boldsymbol{z} \,. \tag{4}$$

Let $\langle\rho\rangle$ be the mean density of the mass within radius R in the galaxy so that $\langle\rho\rangle = 3M(R)/(4\pi R^3)$, where $M(R)$ is the mass of the galaxy within radius R. Then the tidal field components become

$$T_x = \tfrac{4}{3}\pi G(2\langle\rho\rangle - 3\rho)x \,, \tag{5}$$

$$T_y = -\tfrac{4}{3}\pi G\langle\rho\rangle y \,, \tag{6}$$

$$T_z = -\tfrac{4}{3}\pi G\langle\rho\rangle z \,. \tag{7}$$

Thus, the tidal field is always compressive along the directions perpendicular to the radius vector for a spherical potential. It can be either compressive or disruptive along the radius vector depending on the density distribution in the galaxy. For $\rho(R) > 2\langle\rho\rangle/3$ the tidal field is compressive. The nature of the tidal field thus depends on the density profile of the system. For a centrally peaked density profile, the tidal field will always be disruptive along the radial direction. However, if the density profile of the galaxy flattens toward the center, then the tidal field can be compressive within the flat core region of the galaxy. The tidal field is compressive in the centers of clusters of galaxies and is important in the evolution of galaxies in the cluster (Valluri 1993). We show that it is also compressive in the centers of flat-core early-type galaxies and some ultraluminous galaxies; this is derived using equation (2) and is discussed in §§ 3 and 4 of this paper. Equations (5)–(7) are shown to illustrate the physics of compressive tidal fields. For these galaxies the tidal field changes direction from being a disruptive force to a compressive force in the center of the galaxy. We show that this is an important factor in deciding the steady state density of a cloud in the galaxy center.

When the tidal field is compressive along the line of action of the force, the cloud will feel an overall compressive force. In such cases the tidal field can never disrupt the cloud, instead the cloud will be compressed by the galactic field. For a cloud in equilibrium in a compressive tidal field, the internal pressure maintains equilibrium against both the self-gravity of the cloud and the compressive tidal field of the galaxy.

2.2. *Virial Equilibrium of a Cloud*

For a system in virial equilibrium, we have the relation

$$-2\langle K\rangle = \sum_{i=1}^{n} \boldsymbol{F}_i \cdot \boldsymbol{r}_i \,, \tag{8}$$

where $\langle K\rangle$ is the time-averaged kinetic energy of the system, $\boldsymbol{F}_i$ is the force on the ith particle, and $\boldsymbol{r}_i$ is the position coordinate of the ith particle with respect to the cloud center. For a molecular cloud in virial equilibrium, the forces involved will be the internal self-gravity of the cloud and the galactic tidal field acting on the cloud. As mentioned previously, the tidal field is anisotropic. However, for simplicity we will consider only the radial component and not the transverse components of the tidal field in deriving the equilibrium density of a cloud. Strictly speaking we should include all three components of the tidal field which would lead to an ellipsoidal cloud. However, in a real cloud, the compression would tend to become isotropic soon (see § 5). Hence, for simplicity, we assume that the cloud is spherical, and we include only the radial tidal field for estimating the equilibrium cloud density. If we convert the right-hand side of equation (8)

into an integration, we obtain the following relation:

$$-M_c v^2 = -\int \frac{GM_c(r)dM_c(r)}{r} + T_0 \int r^2\, dM_c\,, \qquad (9)$$

where M_c is the mass of the cloud, v is the three-dimensional velocity dispersion in the cloud, and T_0 is the tidal field per unit distance across the cloud (i.e., $T_0 = -\partial^2\Phi/\partial r^2$). We assume that the density within the cloud is inversely proportional to radius as observed (Sanders, Scoville, & Solomon 1985), so that $\rho_c(r) = \rho_0 R_c/r$, where ρ_0 is the density of the cloud at the cloud edge, i.e., at $r = R_c$. Then the cloud has a mass profile given by $M_c(r) = 2\pi R_c \rho_0 r^2$. Thus, the mean density of the cloud, $\langle\rho_c\rangle$, is obtained to be $\langle\rho_c\rangle = 3\rho_0/2$. The equation of cloud equilibrium thus reduces to

$$v^2 = \frac{2}{3}\frac{GM_c}{R_c} - \frac{1}{2}\,T_0\,R_c^2\,. \qquad (10)$$

This has been derived in the galactic rest frame. In the Appendix, we give the derivation in the rest frame of the cloud for the sake of completeness and argue that for considering cloud stability it is appropriate to use the galactic frame equation as derived here.

2.3. *Minimum Density for Stability*

For a tidally disruptive field, the tidal field coefficient T_0 is positive. Since $v^2 > 0$, we obtain the familiar relation for tidal stability of a molecular cloud, namely,

$$\frac{2}{3}\frac{GM_c}{R_c} > \frac{1}{2}\,T_0\,R_c^2\,. \qquad (11)$$

Writing this condition in terms of $\langle\rho_c\rangle$, the mean density of the cloud, we get

$$\langle\rho_c\rangle > \frac{9}{16\pi G}\,T_0\,. \qquad (12)$$

Thus, the minimum density for a cloud to be stable against the disruptive tidal field is

$$\langle\rho_m\rangle = \frac{9}{16\pi G}\,T_0\,. \qquad (13)$$

For a tidally compressive field $T_0 = -|\,T_0\,| < 0$; hence $v^2 > 0$ does not give us any new information except that the cloud can never be disrupted by the tidal field. So to obtain the density of a cloud in the compressive tidal field we impose the condition that the cloud be gravitationally bound to begin with, i.e.,

$$\frac{1}{2}\,v^2 - \frac{2}{3}\frac{GM_c}{R_c} \le 0\,. \qquad (14)$$

Using equation (10) we get

$$\langle\rho_m\rangle = \frac{9}{16\pi G}\,|\,T_0\,|\,, \qquad (15)$$

which is formally the same relation as that for a disruptive tidal field, the only difference being that we take the magnitude of the tidal force coefficient. Physically, however, they have very different significance. For a disruptive field, the minimum density $\langle\rho_m\rangle$ is the density below which a cloud will be disrupted by the galactic tidal field. For a compressive tidal field it denotes the minimum density for a gravitationally bound cloud to exist within that region. Since the cloud is assumed to be gravitationally bound to begin with, an additional inward/compressive field increases the velocity dispersion required to satisfy the virial equilibrium (eq. [10]), and hence the critical density required for stability in presence of a compressive force is actually *higher* for a virialized cloud. For lower densities, the gas within that region will be diffuse and gravitationally unbound. Such gas will not lead to star formation.

We note that the critical number density of hydrogen molecules (in cm^{-3}) corresponding to the mass density $\langle\rho_m\rangle$ (eq. [15]), assuming a 10% gas number fraction in helium, is given by $\langle\rho_m\rangle/(4.68 \times 10^{-24})$. We will use this conversion in the next two sections. To calculate and plot tidal fields, we use mass, length, and time units to be solar masses, parsecs, and 10^7 years, respectively. This means that the units of T_0 are $(10^7\ \mathrm{yr})^{-2}$.

3. APPLICATION TO MOLECULAR GAS IN EARLY-TYPE GALAXIES

In this section we apply the above criterion to predict the central molecular gas densities in six early-type galaxies. As mentioned later in this section, we need parameters that can be derived from the luminosity profile. Unfortunately, only a few of the galaxies whose surface brightness has been studied have also been detected in CO. Hence, we could apply the results of the previous section to only a small sample of early-type galaxies.

3.1. *Spherical Stellar Potential*

Tremaine et al. (1994) have derived a one-parameter set of models for spherical stellar systems. These give self-consistent potential-density pairs. Their model can be applied to the center of early-type galaxies and spiral bulges. From their model they derive the density distribution, surface brightness profile, and line-of-sight velocity dispersion. For all the models, at large distances the density distribution tends to $\rho(r) \propto r^{-4}$, and the surface brightness tends to the familiar $r^{1/4}$ form. The family of potentials, called η models, are given by

$$\Phi(r') = \frac{GM_g}{R_0}\,\frac{1}{(\eta-1)}\left[\frac{r'^{(\eta-1)}}{(1+r')^{\eta-1}} - 1\right], \qquad (16)$$

where $r' = R/R_0$, $0 < \eta \le 3$, M_g is the mass of the galaxy, and R_0 is the core radius. Many of the properties of the η models have also been derived by Dehnen (1993). The $\eta = 1$ model corresponds to the Jaffe (1983) model, while the $\eta = 2$ model corresponds to the Hernquist (1990) model. From equation (16), T_0, the tidal field per unit distance is found to be

$$T_0 = -\frac{GM_g}{R_0}\,\frac{r'^{(\eta-3)}}{(1+r')^{\eta+1}}\,(\eta - 2 - 2r')\,. \qquad (17)$$

For $0 < \eta \le 2$ the density diverges toward the center of the galaxy, and the tidal field is always disruptive. In contrast, for $2 < \eta \le 3$ the model has a more flat density core, and the tidal field is compressive within the core. However, even here, the field is compressive only for distances $R < R_0/2$.

Thus, to determine the critical density in the centers of these galaxies we need to determine two parameters; one is M_g, the mass of the galaxy, which can be determined from the mass-to-luminosity ratio (M/L_v), and the other is the observed core or break radius R_0. The break radius can be

determined from the surface brightness profile of the galaxy. For a flat-core profile the break radius is very sharp, but for a power-law profile, which is rising toward the center, R_0 is not so sharply defined.

3.2. *Results for Minimum Gas Densities*

There are now a very large number of early-type galaxies with detected H_2 gas (Knapp 1998; Henkel & Wiklind 1997). In fact, after looking at the literature, we found that there are over 50 elliptical and S0 galaxies with detected H_2 gas. Many show both CO (1–0) and CO (2–1) lines toward the center indicating that there may be fairly dense gas in these galaxies. The fact that dense gas does exist in many early-type galaxies indicates that there must be some stabilizing mechanism resulting in fairly long-lived dense gas in the centers of these galaxies.

In this section we use the results of the previous section to explain the observed molecular gas densities in a sample of elliptical and S0 galaxies. To determine $\langle \rho_m \rangle$ we need both the galaxy mass and the break radius to apply the analytical models of Tremaine et al. (1994). These parameters have been determined for a large sample of early-type galaxies by Faber et al. (1997). They used very high-resolution *HST* observations to determine the central parameters of 61 early-type galaxies. We compared their sample with CO observations of elliptical galaxies in the literature. We found that molecular gas has been detected in the center of only a few of the galaxies in the Faber et al. (1997) sample. We have used the data in columns (3) and (5) of Table 3 in Faber et al. (1997) to determine the mass of the galaxy M_g, and we used the data in Table 2 of their paper to determine the break or core radius R_0 of the galaxy. The results are shown in Table 1, where we have listed the galaxies, the parameters R_0 and M_g, and the density of molecular gas predicted from equation (15) of the previous section. Figure 1 illustrates how the tidal field varies in a power-law galaxy (NGC 4697) and in a core profile galaxy (NGC 4649). For the latter, the tidal field becomes negative, i.e., compressive within a certain radius in the galaxy, while for NGC 4649 the tidal field continues to rise toward the center. Figure 2 shows the variation of minimum density in the disruptive and compressive tidal regions of NGC 4472. The dashed line demarcates the regions of the compressive and disruptive tidal field. In the following paragraphs, we have compared our results with the CO observations of the sample of galaxies taken from Faber et al. (1997).

NGC 4594 and NGC 4697.—Both these galaxies have power-law profiles and thus the tidal field is always disruptive in both of them. NGC 4594 (also called the "Sombrero Galaxy") has a very steep brightness profile in the center and also has an active nucleus (Bajaja et al. 1988). Bajaja et al. (1991) observed this galaxy in the CO (1–0) and (2–1) line, and although they detected CO in the disk of the galaxy, they could not detect any CO in the center. The reason for this could be that the tidal field is very high in the inner few hundred parsecs and the gas cannot survive there. NGC 4697, on the other hand, has a moderately steep luminosity profile, with a break radius of $\sim$240 pc (Faber et al. 1997). Using $\eta = 1.5$ in equation (17) we get the tidally limited density to be $\langle n \rangle > \sim 5 \times 10^2$ cm^{-3} at 1 kpc, and it rises to $\langle n \rangle \sim 10^5$ cm^{-3} at 200 pc. Sofue & Wakamatsu (1993) have detected CO emission from the central 1 kpc of this galaxy. Since the mass profile does not rise very steeply in the center of this galaxy, the tidal field is not very strong and so gas can exist in the center of NGC 4697 even though

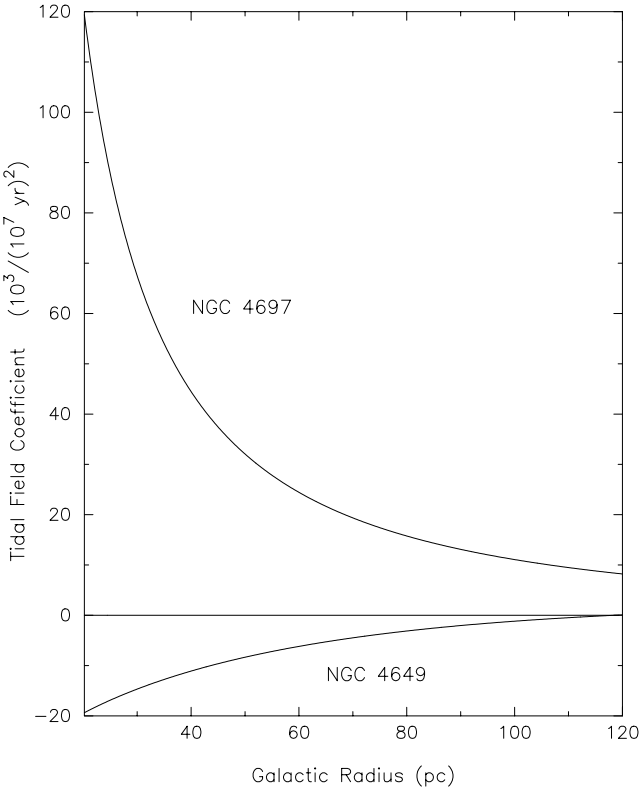

FIG. 1.—Plot of tidal field per unit mass vs. radius (pc) for a power-law early-type galaxy (NGC 4697) where the field is disruptive at all radii, and for a core-profile galaxy (NGC 4649) where the field becomes compressive inside a radius of $\sim$130 pc.

TABLE 1

MODEL CLOUD DENSITIES FOR EARLY-TYPE GALAXIES

Galaxy Name	Galaxy Type	Core/Power Law Type	Break Radius R_0 (pc)	Galaxy Mass ($M_\odot$)	Predicted H_2 Number Density (cm^{-3}) at $R' = 0.4$
NGC 4594.....	Sa/Sb	Power law	4	1.1×10^{11}	...
NGC 4697.....	E6	Power law	240	1.5×10^{11}	...
NGC 4472.....	E/S0	Flat core	178	8.4×10^{11}	10^4
NGC 4649.....	E1-2	Flat core	263	9.9×10^{11}	5×10^3
NGC 1400.....	E1/S0	Flat core	35	2.4×10^{11}	5×10^6
NGC 1316.....	S0	Flat core	36	2.9×10^{11}	5×10^5
NGC 1600.....	E	Flat core	759	1.5×10^{12}	300
NGC 3379.....	E	Flat core	83	9.8×10^{10}	10^4
NGC 4486.....	E	Flat core	562	9×10^{11}	420

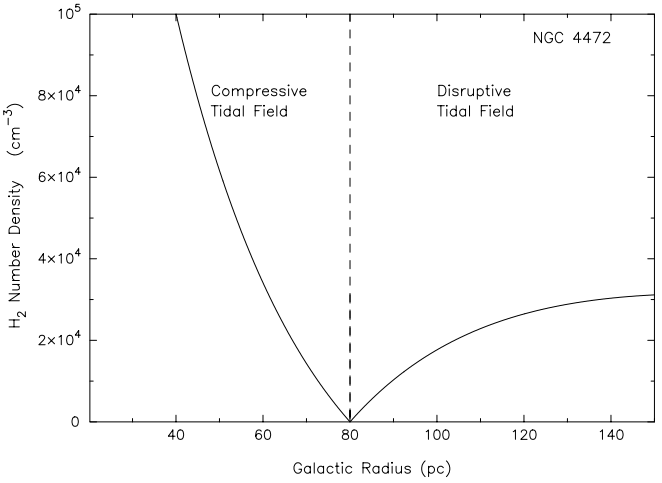

FIG. 2.—Steady state number density for molecular hydrogen gas in bound, virialized clouds vs. radius (pc) for NGC 4472. Note that the dashed line separates the outer region of disruptive tidal field from the inner region of compressive tidal field.

it has a power-law profile like NGC 4594. We do not address the origin of high-density gas observed in some power-law galaxies.

NGC 4472.—This galaxy has a flat-core luminosity profile and hence the tidal field is compressive in the center. The break radius is ~ 180 pc, which means that gas will feel the compressive tidal field within the inner 100 pc, where densities of at least $\langle n \rangle \sim 10^4$ cm^{-3} are predicted by equation (15). CO emission detection indicates that there is $\sim 10^7\ M_\odot$ of molecular gas in this galaxy (Huchtmeier et al. 1994; Lees et al. 1991). However, Huchtmeier et al. (1988) could only detect CO from an off-center position and not at the center. One reason for this could be that their beam was very large (~ 2 kpc). Higher resolution observations might lead to detection of high-density gas in the center of this galaxy.

NGC 4649.—This galaxy is a giant elliptical belonging to the Virgo cluster. It has a fairly large core which is compressive at radii less than 130 pc. The model predicts gas densities of at least $\langle n \rangle \sim 5 \times 10^3$ cm^{-3} in the inner 130 pc. CO (2–1) and CO (1–0) emission has been detected from this galaxy (Lees et al. 1991; Sage & Wrobel 1989).

NGC 1400 and NGC 1316.—These galaxies both have small cores, and the model predicts stable gas of densities of at least $\langle n \rangle > \sim 10^5$–$10^6$ cm^{-3} in the central 10–20 pc of these galaxies. If the galaxy had a power-law profile, the gas would probably not be stable so close to the center. CO emission has been detected from NGC 1400 by Lees et al. (1991) and in NGC 1316 by Sage & Galletta (1993).

NGC 1600, NGC 3379, and NGC 4486.—These galaxies have not been detected in CO; only upper limits to their molecular gas masses have been obtained (Sofue & Wakamatsu 1993). All three galaxies are ellipticals with compressive cores, and hence dense gas can exist in the inner 100 pc of their cores.

4. APPLICATION TO MOLECULAR GAS IN ULTRALUMINOUS GALAXIES

Ultraluminous galaxies are merger remnants with large amounts of molecular gas concentrated in their centers. Over the past few years observations have revealed that the nuclear molecular gas is located in a central disk of size smaller than a few hundred parsecs (Scoville et al. 1991; Downes, Solomon, & Radford 1993). Downes & Solomon (1998) observed with high resolution a sample of ultraluminous galaxies and showed that most of the CO flux from the center comes from subthermally excited CO emission. They concluded that most of the gas is of density $\sim 10^3$ cm^{-3}, and only $\sim 25\%$ of it is high-density gas ($\geq 10^4$ cm^{-3}). We use our model to determine the minimum density of bound, virialized molecular gas clouds for their sample of galaxies using their parameters for the rotation curves and show that our resulting values compare well with their observations. Despite the high observed turbulent velocities (see Table 5 of Downes & Solomon 1998), the assumption of an individual cloud being bound may still be applicable if the beam covers a number of clouds, and hence a large fraction of the line width is due to cloud-cloud velocity dispersion. Also, the volume filling factor of the central molecular gas is ~ 1. Nevertheless, we have treated the central gas as being discrete bound clouds for simplicity.

4.1. *Tidal Field from the Nuclear Rotation Curve*

Downes & Solomon (1998) have observed the rotation curves of the molecular gas disks in a sample of 10 ultraluminous galaxies. They found that the rotation curves rose to a steady velocity V_0 at a radius R_d and then became flat at the steady value. They modeled the rotation curves with the simple expression

$$V_r(R) = V_0 \left(\frac{R}{R_d} \right)^\beta , \tag{18}$$

where $\beta = 1$ for $R < R_d$ and $\beta = 0$ for $R \geq R_d$ up to the maximum radius at which CO was observed.

For the power-law rotation curve (for $R < R_d$), the corresponding potential can be calculated to be

$$\psi(R) = \frac{V_0^2}{2\beta} \left(\frac{R}{R_d} \right)^{2\beta} . \tag{19}$$

Hence, T_0, the tidal field along the radial direction is obtained to be

$$T_0 = -(2\beta - 1) \frac{V_0^2}{R_d^2} . \tag{20}$$

We note that $T_0 < 0$, that is the radial component of the tidal field is compressive, when $\beta > \frac{1}{2}$. Therefore, for $\beta = 1$ as seen in the inner regions of ultraluminous galaxies, the galactic tidal field is compressive. For the region outside of R_d, where the rotation curve is flat, the galactic tidal field is not compressive; instead it is disruptive.

In Figure 3, we show the plot of the tidal field per unit mass versus the galactic radial distance for Arp 193 for the data from Downes & Solomon (1998). The tidal field is compressive inside of 220 pc. Note that sharp transition from disruptive to compressive region is an artifact due to the rotation curve model obtained by Downes & Solomon (1998), the actual transition is probably smoother.

4.2. *Results for Minimum Gas Densities*

We used equations (15) and (20) to determine the minimum density for a bound, virialized cloud to exist in the compressive tidal field of the ultraluminous galaxies observed by Downes & Solomon (1998). Our results are

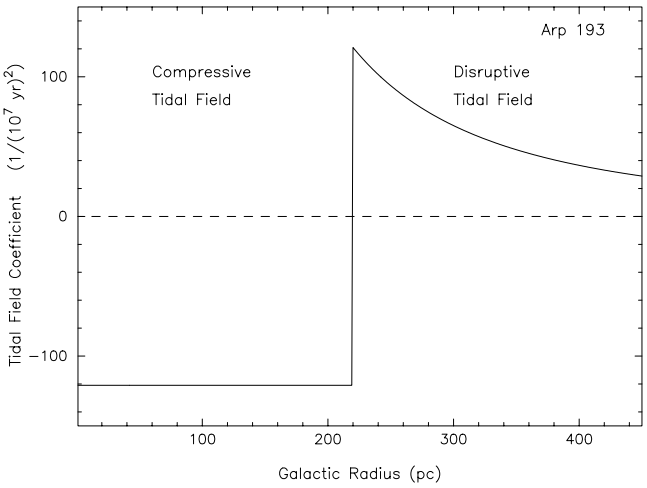

FIG. 3.—Plot of tidal field per unit mass vs. radius (pc) for an ultraluminous galaxy Arp 193. The field becomes compressive inside a radius of 220 pc. The sharp transition is an artifact due to the rotation curve model adopted.

shown in Table 2, where we have listed the galaxies, their rotation curve turnover velocity, turnover radius, and the minimum gas density $\langle \rho_m \rangle$. The particle number density $\langle n \rangle$ lies in the range 10^2–10^4 cm^{-3}. This density is the *minimum* density of a gravitationally bound cloud to remain stable in the center of the galaxy. This range agrees very well with the mean density of the main mass component of the molecular gas observed in these galaxies (see Table 6 of Downes & Solomon 1998). Since we have assumed discrete clouds with a volume filling factor of less than 1 (§ 4), our values are slightly larger than the observed values, as expected, since the latter have been derived assuming a uniformly filled disk.

The peak density of the molecular gas is observed to be near the turnover point in the rotation curve whereas our model predicts a constant high density inside this point. Also there is substantial gas observed beyond the turnover point, but both these could arise because of the sharp turnover in the model rotation curve assumed by Downes & Solomon (1998).

We note that the very dense gas with $n \geq 10^4$ cm^{-3}, which constitutes about 25% of the gas mass in the extreme starburst regions such as Arp 220 west and east, could also arise due to tidal compression (see Table 12 of Downes & Solomon 1998 and our Table 2). This high-density gas is the site of HCN emission and contains a large fraction of the star formation. Since the internal velocity dispersion increases with density for a bound virialized cloud, the observed velocity dispersion in a given region sets an upper limit on the high density that can result from this mechanism. The observed dispersion in a region could be due to the superposition of a number of moderate-density clouds ($\langle n \rangle \sim 10^2$–$10^4$ cm^{-3}) in the beam, as we argued in § 4, or it could be due to a few higher density clouds. We do not discuss the issues of the fraction of the gas in the dense component, and the origin of the high central turbulent velocities, in this paper.

It is interesting that even low- to moderate-density gas $\langle n \rangle \sim 10^2$–$10^3$ cm^{-3} in some cases can survive in the center and will not be disrupted by the galactic tidal shear. Downes & Solomon (1998) suggest that most of the moderate-density gas (10^3 cm^{-3}) that they observe in these galaxies is diffuse and unbound as it may not be able to withstand the tidal shear of the nuclear region of the galaxy. However, as we have shown here, gas can survive near the center as bound clouds because the tidal field is compressive and not disruptive. Hence, the gas that they have termed as the "diffuse medium" could well be bound clouds.

Since these clouds are bound, they are more susceptible to the onset of star formation. Thus, our conclusion that these clouds are bound helps the scenario proposed by Downes & Solomon (1998) for starbursts powering the ultraluminous galaxies. The starbursts could be triggered due to large-scale gravitational star-gas instability (Jog 1996), as they suggest, and/or it could arise due to the collapse of the individual, bound clouds, or due to collisions between the bound clouds. Hence, the formation of dense gas ($\langle n \rangle \geq 10^2$–$10^4$ cm^{-3}) in a compressive tidal field is important for the starburst and hence the evolution of ultraluminous galaxies.

5. DISCUSSION

1. Normal spirals also show dense gas in their central regions (e.g., Henkel, Baan, & Mauersberger 1991), so it is natural to ask if one could apply the above analysis and obtain the resulting steady state density of the dense, virialized clouds. Carollo & Stiavelli (1998) have observed the nuclear surface brightness profile of a large sample of spiral galaxies using *HST*. A considerable fraction of these spirals have a flat-core luminosity profile close to their center. The

TABLE 2

MODEL CLOUD DENSITIES FOR ULTRALUMINOUS GALAXIES

Galaxy Name	Rotation Curve Turnover Radius (pc)	Rotation Curve Turnover Velocity (km s^{-1})	Predicted H_2 Number Density (cm^{-3})
00057+4021.....	240	250	7×10^2
02483+4302.....	270	270	6×10^2
VII Zw 31	290	290	6×10^2
10565+2448.....	230	220	6×10^2
Mrk 231	75	345	10^4
Arp 193-disk	220	230	7×10^2
Mrk 273-disk.....	70	280	10^4
Arp 220-disk	200	330	2×10^3
Arp 220-west	35	300	5×10^4
Arp 220-east.....	50	350	3×10^4
17208-0014	310	260	5×10^2
23365+3604.....	340	260	4×10^2

galactic tidal field for these galaxies can become compressive within the core. We plan to study these galaxies in further detail in a forthcoming paper. In particular, we would like to examine how the molecular cloud densities in these galaxies compare with those predicted by our work. This may help us decide whether the so-called diffuse, intercloud medium in normal and starburst galaxies (e.g., Bally et al. 1988; Jog & Das 1992) actually consists of bound, virialized clouds.

2. However, the mass distribution and hence the dynamics in the centers of spirals is more complex due to the common presence of bars and triaxial bulges. We find that for the Milky Way galaxy, assuming the bar potential as in Binney et al. (1991), the field is not compressive. A typical bulge potential (e.g., Sellwood & Wilkinson 1993) also does not result in compressive fields. Physically, this could be because a bar is a strong deviation from an axisymmetric potential, and the field near the bar is not smooth. In fact, for a molecular cloud close to a strong bar, the galactic tidal field is shown to cause an internal heating of the cloud (Das & Jog 1995). We will discuss the barred case in a future paper.

3. We have only considered the radial tidal field in this paper. The tidal fields along the other two orthogonal directions are always compressive (see § 2.1) and have magnitudes comparable to the radial case. We are justified in neglecting this asymmetry since the gas clouds are compressible and would tend to have an isotropic velocity dispersion, and hence the net effect of the compressive fields would be seen in an average sense. In the case of the ultraluminous galaxies, this asymmetry would be particularly stronger since the height of the disk is small, and hence using a three-dimensional distribution is not strictly correct.

4. In the centers of ultraluminous galaxies, the gas constitutes a significant fraction of the mass ($\geq 25\%$) and hence the gravitational potential. Thus, a gas cloud does not respond to the stellar potential alone. Since we have used the observed gas rotation curve in obtaining the potential, we have used the potential as seen by a gas cloud.

6. CONCLUSIONS

We have investigated a simple but novel physical process which can compress gravitationally bound, virialized molecular clouds in the centers of galaxies. The main conclusions of this study are the following.

1. The galactic tidal field changes from being disruptive to compressive in the centers of flat-core early-type galaxies and ultraluminous galaxies.

2. The compressive tidal force and the self-gravity of the cloud are balanced by the internal pressure of the cloud. We have used the virial theorem to derive a simple expression for the minimum mean density of a gravitationally bound cloud in the compressive core of a galaxy. The additional inward/compressive field increases the velocity dispersion required to satisfy the virial equilibrium, and hence the critical density required for stability in presence of a compressive force is *higher* for a gravitationally bound, virialized cloud. For lower densities, the gas within that region will be diffuse and gravitationally unbound. Such gas will not lead to star formation.

3. We have applied our results to a sample of flat-core, early-type galaxies taken from Faber et al. (1997). The gas densities predicted by the model varies with core size and cloud position in the center of the galaxy, and the typical density range observed within the central 100 pc is $\langle n \rangle \sim 10^3$–$10^6$ cm^{-3}. The galaxies in our sample were chosen so that they have an observational evidence of molecular gas in their centers. However, the spatial resolution of these data are not yet adequate and only give a beam-averaged lower limit on the gas densities. Future high-resolution studies of such galaxies are highly recommended.

4. We have also applied our results to the molecular gas disks observed in the centers of ultraluminous galaxies (Downes & Solomon 1998). From their observed rotation curves, we show that they have a compressive core within their central region. The minimum mean molecular cloud densities predicted from our model are in the range of 10^2–10^4 cm^{-3}, and this range matches well with the observed gas densities in these galaxies. Also, if the tidal field is compressive and not disruptive as previously thought in the literature, this molecular gas can exist in the form of bound clouds. Hence, these clouds are closer to star formation than unbound, diffuse molecular gas. This strengthens the scenario proposed by Downes & Solomon (1998) for starbursts powering the ultraluminous galaxies.

M. D. would like to thank R. Nityananda for useful discussions during the course of this work, and we would like to thank M. Valluri and S. Faber for very useful e-mail correspondence regarding this work. We thank the anonymous referee for helpful comments which improved the comparison with observations of ultraluminous galaxies. We thank S. Sridhar for comments on the choice of reference frame, which we have addressed in the Appendix.

APPENDIX

CLOUD EQUILIBRIUM IN THE INERTIAL AND ROTATING FRAMES

In this Appendix we derive the condition of cloud stability (see eq. [10]) in the galactic reference frame and in the rotating frame moving with the cloud. We then discuss which equation was used in the paper and the reasons behind choosing that particular form. The coordinate of the cloud with respect to the center of the galaxy is $\boldsymbol{R}_0$. The ith clump in the cloud has a position coordinate $\boldsymbol{R}_i$ with respect to the galaxy center and $\boldsymbol{r}_i$ with respect to the cloud center, so that $\boldsymbol{R}_i = \boldsymbol{R}_0 + \boldsymbol{r}_i$. The number of clumps in the cloud is n so that the index $i = 1$ to n.

Galactic frame.—The origin of the coordinate system is the center of the galaxy. For the ith clump within the cloud the total velocity $\boldsymbol{V}_{ig}$ is given by

$$\boldsymbol{V}_{ig} = \boldsymbol{V}_0 + \boldsymbol{v}_i \,, \tag{A1}$$

where $\boldsymbol{V}_0$ is the rotational velocity of the cloud about the galaxy center and $\boldsymbol{v}_i$ is the random motion of the ith clump. The kinetic energy of the cloud K, is given by

$$2K = M_c V_0^2 + \sum_{i=1}^{n} m_i v_i^2 + 2\boldsymbol{V}_0 \cdot \left(\sum_{i=1}^{n} \boldsymbol{p}_i \right). \tag{A2}$$

But when the last term is averaged over time, the random velocities of the clumps makes the term average out to zero. Hence, equation (A2) reduces to

$$2\langle K \rangle = M_c V_0^2 + \left\langle \sum_{i=1}^{n} m_i v_i^2 \right\rangle . \tag{A3}$$

To determine the right-hand side of equation (8), we first determine the force on the ith clump, which is the sum of the galactic potential and the self-gravity of the cloud:

$$\boldsymbol{F}_i = -\left(\frac{\partial \Phi}{\partial R} \right)_i m_i \hat{\boldsymbol{R}}_i - \sum_{j=1}^{n} \frac{G m_i m_j}{|\boldsymbol{r}_{ij}|^3} \boldsymbol{r}_{ij} , \tag{A4}$$

where $\boldsymbol{r}_{ij} = (\boldsymbol{r}_i - \boldsymbol{r}_j)$. Expanding the force term $(\partial\Phi/\partial R)_i$ about the radius R_0 gives the tidal term so that $\sum_{i=1}^{n} \boldsymbol{F}_i \cdot \boldsymbol{r}_i$ reduces to

$$\sum_{i=1}^{n} \boldsymbol{F}_i \cdot \boldsymbol{r}_i = -\frac{V_0^2}{R_0^2} \hat{\boldsymbol{R}}_i \cdot \sum_{i=1}^{n} m_i \boldsymbol{r}_i + T_0 \sum_{i=1}^{n} m_i r_i^2 - \sum_{\substack{i=1, \\ i \neq j}}^{n} \sum_{\substack{j=1, \\ i \neq j}}^{n} \frac{G m_i m_j}{|\boldsymbol{r}_{ij}|} . \tag{A5}$$

Using the relation $M_c \boldsymbol{R}_0 = \sum_{i=1}^{n} m_i \boldsymbol{r}_i$, the equation of virial equilibrium for the cloud reduces to

$$\left\langle \sum_{i=1}^{n} m_i v_i^2 \right\rangle = \sum_{\substack{i=1, \\ i \neq j}}^{n} \sum_{\substack{j=1, \\ i \neq j}}^{n} \frac{G m_i m_j}{|\boldsymbol{r}_{ij}|} - T_0 \left\langle \sum_{i=1}^{n} m_i r_i^2 \right\rangle . \tag{A6}$$

We have used this form of the virial equation (see eq. [10]) to determine the minimum cloud density in a compressive tidal field.

Rotating frame.—In this case the coordinate system is centered in the cloud so that the ith clump has a position vector $\boldsymbol{r}_i$. The force in the rotating frame is given by

$$\boldsymbol{F}_i = -m_i \left(\frac{\partial \Phi}{\partial R} \right)_i \hat{\boldsymbol{R}}_i - \sum_{j=1}^{n} \frac{G m_i m_j}{|\boldsymbol{r}_{ij}|^3} \boldsymbol{r}_{ij} - 2m_i(\boldsymbol{\omega}_0 \times \boldsymbol{v}_{ri}) - m_i \boldsymbol{\omega}_0 \times (\boldsymbol{\omega}_0 \times \boldsymbol{R}_i) , \tag{A7}$$

where $\boldsymbol{\omega}_0$ is rotation velocity of the cloud about the galaxy center, i.e., $|\boldsymbol{\omega}_0| = V_0/R_0$, and $\boldsymbol{v}_{ri}$ is the random motion of the ith clump in the rotating frame. The third term on the right-hand side of the equation is the Coriolis force, and the fourth term is the centrifugal force. We expand the force term $(\partial\Phi/\partial R)_i$ about R_0 and put $\boldsymbol{R}_i = \boldsymbol{R}_0 + \boldsymbol{r}_i$. Since $(\partial\Phi/\partial R)_0 = \omega_0^2 R_0$ and $\boldsymbol{\omega}_0 \times (\boldsymbol{\omega}_0 \times \boldsymbol{R}_0) = -\omega_0^2 R_0 \hat{\boldsymbol{R}}_0$, the force $\boldsymbol{F}_i$ becomes

$$\boldsymbol{F}_i = T_0 m_i \boldsymbol{r}_i - \sum_{j=1}^{n} \frac{G m_i m_j}{|\boldsymbol{r}_{ij}|^3} \boldsymbol{r}_{ij} - 2m_i(\boldsymbol{\omega}_0 \times \boldsymbol{v}_{ri}) - m_i \boldsymbol{\omega}_0 \times (\boldsymbol{\omega}_0 \times \boldsymbol{r}_i) . \tag{A8}$$

Hence, $\boldsymbol{F}_i \cdot \boldsymbol{r}_i$ is given by

$$\boldsymbol{F}_i \cdot \boldsymbol{r}_i = T_0 m_i r_i^2 - \sum_{j=1}^{n} \frac{G m_i m_j}{|\boldsymbol{r}_{ij}|^3} \boldsymbol{r}_{ij} \cdot \boldsymbol{r}_i - 2m_i(\boldsymbol{\omega}_0 \times \boldsymbol{v}_{ri}) \cdot \boldsymbol{r}_i - m_i \boldsymbol{\omega}_0 \times (\boldsymbol{\omega}_0 \times \boldsymbol{r}_i) \cdot \boldsymbol{r}_i . \tag{A9}$$

Now, $\boldsymbol{\omega}_0 \times (\boldsymbol{\omega}_0 \times \boldsymbol{r}_i) \cdot \boldsymbol{r}_i = -(\boldsymbol{\omega}_0 \times \boldsymbol{r}_i)^2$ and $(\boldsymbol{\omega}_0 \times \boldsymbol{v}_{ri}) \cdot \boldsymbol{r}_i = -\boldsymbol{\omega}_0 \cdot (\boldsymbol{r}_i \times \boldsymbol{v}_{ri})$. So equation (A9) becomes

$$\boldsymbol{F}_i \cdot \boldsymbol{r}_i = T_0 m_i r_i^2 - \sum_{j=1}^{n} \frac{G m_i m_j}{|\boldsymbol{r}_{ij}|^3} \boldsymbol{r}_{ij} \cdot \boldsymbol{r}_i + 2\boldsymbol{\omega}_0 \cdot (m_i \boldsymbol{r}_i \times \boldsymbol{v}_{ri}) + m_i(\boldsymbol{\omega}_0 \times \boldsymbol{r}_i)^2 . \tag{A10}$$

Also, $\boldsymbol{L}_i = m_i(\boldsymbol{r}_i \times \boldsymbol{v}_i)$ is the angular momentum of the clump measured in the inertial or galactic frame, and $\boldsymbol{L}_{ir} = m_i(\boldsymbol{r}_i \times \boldsymbol{v}_{ri})$ is the cloud angular momentum as measured in the rotating frame. The two are related through the following relations (e.g., Goldstein 1980):

$$\boldsymbol{V}_{ig} = \boldsymbol{v}_{ri} + \boldsymbol{\omega}_0 \times \boldsymbol{R}_i . \tag{A11}$$

Since $\boldsymbol{V}_{ig} = \boldsymbol{V}_0 + \boldsymbol{v}_i$, $\boldsymbol{R}_i = \boldsymbol{R}_0 + \boldsymbol{r}_i$ and $\boldsymbol{V}_0 = \boldsymbol{\omega}_0 \times \boldsymbol{R}_0$, we obtain the relation,

$$\boldsymbol{\omega}_0 \cdot \boldsymbol{L}_i = \boldsymbol{\omega}_0 \cdot \boldsymbol{L}_{ir} + m_i(\boldsymbol{\omega}_0 \times \boldsymbol{r}_i)^2 . \tag{A12}$$

However, observations indicate that clouds are practically nonrotating, so the net angular momentum of a cloud $\sum_i \boldsymbol{L}_i$ as observed in the inertial frame is ~ 0 (Blitz 1991). Applying this to equation (A10) we get the following relation:

$$\sum_i \langle v_{ri}^2 \rangle = \sum_{\substack{i=1, \\ i \neq j}}^{n} \sum_{\substack{j=1, \\ i \neq j}}^{n} \frac{G m_i m_j}{|\boldsymbol{r}_{ij}|} - T_0 \sum_{i=1}^{n} m_i r_i^2 + \sum_{i=1}^{n} m_i(\boldsymbol{\omega}_0 \times \boldsymbol{r}_i)^2 . \tag{A13}$$

So the equation of equilibrium is different from that in the inertial or galactic frame by one term (see eq. [A6]). However, using the relation $v_{ri}^2 = (\boldsymbol{v}_i - \boldsymbol{\omega}_0 \times \boldsymbol{r}_i)^2$, we obtain,

$$\sum_i m_i v_{ri}^2 = \sum_i m_i v_i^2 + \sum_i m_i(\boldsymbol{\omega}_0 \times \boldsymbol{r}_i)^2 \ , \tag{A14}$$

which when substituted in equation (A13) leads to an identical relation for cloud equilibrium as obtained in the galactic frame and as expected physically.

We have chosen to use the Galactic or inertial frame equation (A6) and not equation (A13) simply because the velocity is observed from the galactic reference frame and not from within the cloud (which is the rotating frame). Hence, we use the velocity dispersion $\langle \sum_i v_i^2 \rangle$ and not $\langle \sum_i v_{\rm ri}^2 \rangle$.

REFERENCES

Bajaja, E., Dettmar, R. J., Hummel, E., & Wielebinski, R. 1988, A&A, 202, 35
Bajaja, E., Krause, M., Dettmar, R. J., & Wielebinski, R. 1991, A&A, 241, 411
Bally, J., Stark, A. A., Wilson, R. W., & Henkel, C. 1988, ApJ, 324, 223
Barnes, J. E., & Hernquist, L. 1992, ARA&A, 30, 705
Binney, J., Gerhard, O. E., Stark, A. A., Bally, J., & Uchida, K. I. 1991, MNRAS, 252, 210
Binney, J., & Tremaine, S. 1987, Galactic Dynamics (Princeton: Princeton Univ. Press)
Blitz, L. 1991, The Physics of Star Formation and Early Stellar Evolution, ed. C. J. Lada & N. D. Klyafis (Dordrecht: Kluwer), 3
Carollo, C. M., & Stiavelli, M. 1998, AJ, 115, 2306
Cowsik, R., & Ghosh, P. 1987, ApJ, 317, 26
Das, M., & Jog, C. J. 1995, ApJ, 451, 167
Dehnen, W. 1993, MNRAS, 265, 250
Downes, D., & Solomon, P. M. 1998, ApJ, 507, 615
Downes, D., Solomon, P. M., & Radford, S. J. E. 1993, ApJ, 414, L13
Faber, S. M., et al. 1997, AJ, 114, 1771
Goldstein, H. 1980, Classical Mechanics (New York: Addison-Wesley)
Henkel, C., Baan, W. A., & Mauersberger, R. 1991, Astron. Astrophys. Rev., 3, 47
Henkel, C., & Wiklind, T. 1997, Space Sci. Rev., 81, 4
Hernquist, L. 1990, ApJ, 356, 359
Huchtmeier, W. K., Bregman, J. N., Hogg, D. E., & Roberts, M. S. 1988, A&A, 198, L17
———. 1994, A&A, 281, 327
Jaffe, W. 1983, MNRAS, 202, 995
Jog, C. J. 1996, MNRAS, 278, 209
Jog, C. J., & Das, M. 1992, ApJ, 400, 476
Knapp, G. R. 1998, in ASP Conf. Proc. 163, Star Formation in Early-Type Galaxies, ed. P. Carral & J. Cepa (San Francisco: ASP), 1
Kormendy, J., & Sanders, D. B. 1992, ApJ, 390, L53
Lees, J. F., Knapp, G. R., Rupen, M. P., & Phillips, T. G. 1991, ApJ, 379, 177
Ostriker, J. P., Spitzer, L., & Chevalier, R. A. 1972, ApJ, 176, L51
Sage, L. J., & Galletta, G. 1993, ApJ, 419, 544
Sage, L. J., & Wrobel, J. M. 1989, ApJ, 344, 204
Sanders, D. B., & Mirabel, I. F. 1996, ARA&A, 34, 749
Sanders, D. B., Scoville, N. Z., & Solomon, P. M. 1985, ApJ, 289, 373
Sanders, D. B., Soifer, B. T., Elias, J. H., Madore, B. F., Matthews, K., Neugebauer, G., & Scoville, N. Z. 1988, ApJ, 325, 74
Schweizer, F. 1999, in IAU Symp. 186, Galaxy Interactions at Low and High Redshift, ed. D. B. Sanders & J. E. Barnes (Dordrecht: Kluwer), 1
Scoville, N. Z., Sargent, A. I., Sanders D. B., & Soifer, B. T. 1991, ApJ, 366, L5
Sellwood, J., & Wilkinson, A. 1993, Rep. Prog. Phys., 56, 173
Sofue, Y., & Wakamatsu, K. 1993, PASJ, 45, 529
Solomon, P. M. 1997, in IAU Symp. 170, CO: Twenty-Five Years of Millimeter-Wave Spectroscopy, ed. W. B. Latter, S. J. E. Radford, P. R. Jewell, J. G. Mangum, & J. Bally (Dordrecht: Kluwer), 289
Tremaine, S., et al. 1994, AJ, 107, 634
Valluri, M. 1993, ApJ, 408, 57